JOURNAL OF MATERIALS SCIENCE 9 (1974) 1145–1152

The role of inclusions in the fracture of ceramic materials

A. G. EVANS
Physical Properties Section, National Bureau of Standards, Washington, D.C., USA

The stress concentrations that occur at inclusions due to thermal expansion and elastic modulus mismatch are discussed and the stress intensity factors at interface cracks that result from these stresses are calculated. It is shown that conservative failure prediction based on an equivalence between inclusion size and crack size is usually acceptable if the shear modulus μ or thermal expansion coefficient α for the inclusion is larger than the matrix values. If, however, μ and α are smaller for the inclusion than the matrix, extensive cracking can develop at the inclusions which may lead to premature failure. For this case the only effective methods for failure prediction are techniques which give directly the maximum stress intensity factor, i.e., proof testing and/or acoustic emission.

1. Introduction

Recent studies of fracture in structural ceramic materials have concluded that fracture frequently originates from inclusions, particularly at the critical low strength extreme of the strength distribution [1, 2]. Also, the frequency of fracture incidence from inclusions increases as the component size increases – primarily because the probability of locating an inclusion in the tensile zone increases. Consequently, fracture from inclusions is a major mode of failure in ceramic structural components. An appreciation of the effect of inclusions on the fracture of these materials is thus of critical importance for both strength intepretation and failure prediction. It is intended in this paper to examine the general behaviour of inclusions, and to present analyses which may form the basis of an inclusion classification scheme.

Failure prediction procedures which are cognizant of the effect of inclusions on fracture strength generally involve nondestructive inclusion detection in conjunction with fracture mechanics. Then, in principle, it is possible to identify, and hence discard, any components containing inclusions larger than a certain critical size, a_c. The magnitude of a_c is usually calculated from the maximum service stress and the life expectancy for the component [3, 4] by assuming that the inclusion is equivalent in size to a sharp crack with the same maximum dimension; it is hoped that this will give a conservative estimate of the maximum inclusion size that can be tolerated to ensure satisfactory performance. As yet, however, the relation between inclusion properties and the cracks that are likely to develop prior to fracture in the vicinity of the inclusion has not been established. This problem is examined in this paper in an attempt to identify situations where cracks substantially larger than the inclusion size may form, which might invalidate nondestructive evaluation procedures for structural parts, based solely on inclusion size and assuming inclusion/crack size equivalence, e.g., ultrasonic and radiographic techniques.

2. Stress concentrations around inclusions

Localized stresses can occur around inclusions due to differences in the thermal expansion and the elastic properties of the inclusion and matrix. A difference in thermal expansion coefficient between inclusion and matrix results in spherically symmetric stresses at spherical inclusions [5, 6]. The stresses in the matrix, for an isotropic linear elastic continuum, are given by;*

*Different values for the elastic component of these relations have been reported [7], but these do not affect the spatial distribution of the stresses.

$$\sigma_{rr} = \frac{(\alpha_i - \alpha_m)(T_f - T)}{(1 + \nu_m)/2E_m + (1 - 2\nu_i)/E_i} \equiv -\beta\left(\frac{R}{r}\right)^3 \quad (1)$$

$$\sigma_{\theta\theta} = \frac{(\alpha_m - \alpha_i)(T_f - T)}{2[(1 + \nu_m)/2E_m + (1 - 2\nu_i)/E_i]} \equiv \frac{\beta}{2}\left(\frac{R}{r}\right)^3 \quad (2)$$

where $\alpha_{m,i}$, $\nu_{m,i}$ and $E_{m,i}$ are the expansion coefficients, Poisson's ratio and Young's modulus for the matrix and inclusion, respectively, T_f is the fabrication temperature and T the ambient temperature, R is the inclusion radius, and r is the distance from the centre of the inclusion. The stresses in the inclusion are essentially hydrostatic and given by; $\sigma = \beta$.

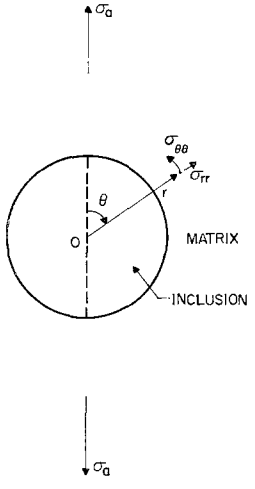

Figure 1 The co-ordinate system used to evaluate the mechanical stresses around inclusions.

A difference in elastic constants between inclusion and matrix results in stress concentrations related to the applied stress, σ_a. These stresses are more complex than the thermal stresses and for simplicity we shall only consider the two dimensional case, i.e., cylindrical inclusions. For this case (Fig. 1), the matrix stresses for a homogeneous system are [8];

$$\sigma_{rr} = \frac{\sigma_a}{2}(1 + \cos 2\theta) + 2\sigma_a\left[-A\left(\frac{R}{r}\right)^2 + B\left[3\left(\frac{R}{r}\right)^4 - 4\left(\frac{R}{r}\right)^2\right]\cos 2\theta\right] \quad (3)$$

$$\sigma_{\theta\theta} = \frac{\sigma_a}{2}(1 - \cos 2\theta) + 2\sigma_a\left[A\left(\frac{R}{r}\right)^2 - 3B\left(\frac{R}{r}\right)^4 \cos 2\theta\right] \quad (4)$$

where,

$$A = \frac{(1 - 2\nu_i)\mu_m - (1 - 2\nu_m)\mu_i}{4[(1 - 2\nu_i)\mu_m + \mu_i]},$$

$$B = \frac{\mu_m - \mu_i}{4[\mu_m + (3 - 4\nu_m)\mu_i]},$$

and

$$A/B = \{1 - 2\nu_i + 2(\mu_i/\mu_m)[4\nu_i\nu_m - \nu_m - 3\nu_i + 1] - (\mu_i/\mu_m)^2[3 - 6\nu_m - 4\nu_i + 8\nu_i\nu_m]\} / [1 - 2\nu_i + 2(\mu_i/\mu_m)\nu_i - (\mu_i/\mu_m)^2]$$

where μ is the shear modulus. In the two limits, i.e., a void, and a rigid inclusion respectively, A is 1/4 and $-(1 - 2\nu_m)/4$ and B is 1/4 and $-1/4(3 - 4\nu_m)$. It is also noted that since $0.15 \lesssim \nu \lesssim 0.35$, then $1 \leqslant A/B \lesssim 1.6$, so that the quantities A and B are always similar in magnitude. The stresses within the inclusion are [8]:

$$\sigma_{rr} = \frac{\sigma_a}{2}(1 + \cos 2\theta) + 2\sigma_a[F/(1 - 2\nu_i) + G\cos 2\theta] \quad (5)$$

$$\sigma_{\theta\theta} = \frac{\sigma_a}{2}(1 - \cos 2\theta) + 2\sigma_a[F/(1 - 2\nu_i) - (G + 6Hr^2)\cos 2\theta] \quad (6)$$

where F, G and H are constants which depend on the elastic constants of the inclusion and matrix.

It is noted that A and B are positive for low modulus inclusions ($\mu_i \lesssim \mu_m$). Hence, for these inclusions, the tangential tensile stresses, $\sigma_{\theta\theta}$, are larger than the applied stress, σ_a, in the orientation $\theta = 90°$; whereas in the orientation $\theta = 0$, the tangential stresses are compressive near the interface, but become tensile further into the matrix. For high modulus inclusions ($\mu_i \gtrsim \mu_m$), A and B are negative. Thus the tangential stresses are still tensile, but $< \sigma_a$, for $\theta = 90°$; whilst the stresses at $\theta = 0$ are tensile near the interface, and become compressive further into the matrix. The radial stress concentrations are much smaller than the tangential and the trends with orientation depend on the relative magnitudes of A and B.

3. Stress intensity factors for interface cracks

The stress concentrations associated with in-

clusions are only likely to affect the fracture behaviour of the host material if cracks develop (comparable in size to the inclusion), due to these stresses, in the vicinity of the inclusion. In brittle materials these cracks could form from small pre-existing defects at, or near, the inclusion/matrix interface. The incidence of crack development will be determined by the magnitude of the stress intensity factor, K, at the small interfacial defects. If K exceeds the critical value K_C for the matrix or inclusion, then the cracks will propagate (and probably arrest) thereby developing into macrocracks. In this section, approximate K values are determined as a function of the interface defect size for the various types of stress concentration considered in the preceding section.

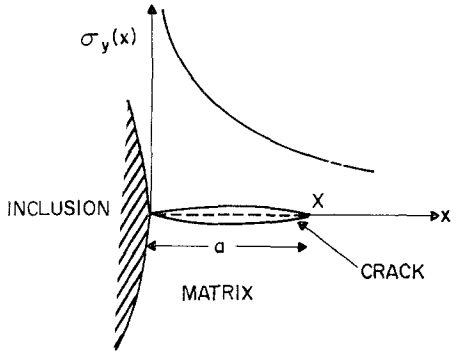

Figure 2 The co-ordinate system used to evaluate the stress intensity factor for a crack in a variable stress field.

The stress intensity factor for a crack in a variable stress field can be determined directly from the orthogonal stress that existed along the fracture plane prior to crack formation [9]. For a through crack of length a [10] (see Fig. 2)

$$K = \left(\frac{2}{a\pi}\right)^{\frac{1}{2}} \int_0^a \frac{\sigma_y(x)x^{\frac{1}{2}}}{(a-x)^{\frac{1}{2}}}\,dx \qquad (7)$$

provided that a is very much smaller than the specimen (component) dimensions. Values for K can thus be evaluated to a first approximation by substituting the stress fields around the inclusions into this relation and integrating over the crack length. This neglects any perturbations of the applied stress field $\sigma_y(x)$ caused by the crack and therefore can only be used as an approximation for small cracks occurring near, or at, the interface ($a \lesssim 0.2R$).

3.1. Thermal stress

When the expansion coefficient for the inclusion is larger than the matrix value, the radial stresses that form while cooling from the fabrication temperature are tensile, $\sigma_{rr} > 0$, and circumferential cracks tends to form, usually in the interface or in the matrix [11]. To a first approximation, therefore, the cracks propagate at constant stress, depending on the location of the defect, and hence K is given simply by:

$$K_T \approx \left(\frac{\pi a}{2}\right)^{\frac{1}{2}} (-\beta)\left(\frac{R}{r}\right)^3 \qquad (8)$$

where the subscript T, denotes the thermal origin of the stress intensity factor.

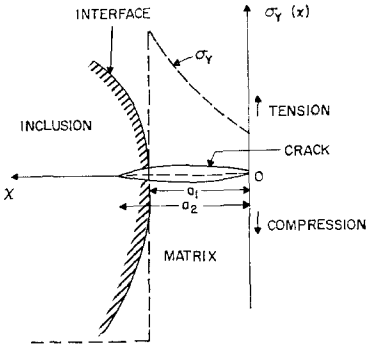

Figure 3 The thermal stresses acting on a crack extending into an inclusion and the co-ordinate system used to estimate the stress intensity factor.

When the expansion coefficient of the inclusion is less than the matrix coefficient, the tangential stresses that develop on cooling are tensile and cracks tend to propagate away from the inclusion through the matrix and, occasionally, through the inclusion (see Fig. 3). The stress intensity factors for cracks adjacent to the interface may be evaluated, to a useful first approximation, if it is considered that the cracks are through cracks exposed along their lengths to the tangential stresses at any equatorial plane through the inclusion (Equation 2). At the end of the crack farthest from the inclusion (x in Fig. 2);

$$K_T = \left(\frac{2}{\pi a}\right)^{\frac{1}{2}} \frac{\beta}{2} \int_0^a \frac{(x/R+1)^{-3}x^{\frac{1}{2}}}{(a-x)^{\frac{1}{2}}}\,dx \cdot \qquad (9)$$

Expanding $(x/R + 1)^{-3}$ as a series and integrating gives;

$$K_T = \frac{\beta}{2}\left(\frac{\pi a}{2}\right)^{\frac{1}{2}}\left[1 - \frac{9}{4}\left(\frac{a}{R}\right) + \frac{15}{4}\left(\frac{a}{R}\right)^2 - \frac{175}{32}\left(\frac{a}{R}\right)^3 + \ldots\right]. \quad (10)$$

The terms beyond (a/R) can, in fact, be neglected because the solution is only valid for small a/R ($\lesssim 0.2$).

If the crack propagates into the inclusion, the part of the crack in the inclusion is under compressive stress (Fig. 3) so that, if we assume an elastic continuum;

$$K_T = \left(\frac{2}{\pi a_2}\right)^{\frac{1}{2}}\left(\frac{\beta}{2}\right)\left[\int_0^{a_1}\frac{(1 + a_1/R - x/R)^{-3}x^{\frac{1}{2}}}{(a_2 - x)^{\frac{1}{2}}}\,dx - 2\int_{a_1}^{a_2}\frac{x^{\frac{1}{2}}}{(a_2 - x)^{\frac{1}{2}}}\,dx\right] \quad (11)$$

where the first term is due to the tensile stresses in the matrix and the second due to the compressive stress in the inclusion. Integration of Equation 11 gives;

$$K_T = \left(\frac{\pi a_2}{2}\right)^{\frac{1}{2}}\frac{\beta}{2}\left(\frac{a_1}{a_2}\right)1 - \frac{3}{4}\left(\frac{a_1}{R}\right)\Bigg] - 2\left(\frac{2a_2}{\pi}\right)^{\frac{1}{2}}\left[(1 - a_1/a_2)^{\frac{1}{2}} - \tan^{-1}(a_2/a_1 - 1)^{\frac{1}{2}}\right] \quad (12)$$

where terms in $(a_1/R)^2$, etc. have been neglected. Hence, as expected, the magnitude of K decreases as the crack extends into the inclusion, and substantial extension into the inclusion is not normally anticipated (unless K_C for the inclusion is abnormally small).

3.2. Mechanical stress

The angular dependence of the mechanical stresses results in a series of solutions for K, depending on crack orientation and location. For simplicity it is considered here that the cracks will be located in the plane of maximum tension, i.e., $\theta = 90°$ for $\mu_m > \mu_i$ and $\theta = 0$ for $\mu_m \ll \mu_i$ (see Fig. 1).

The magnitude of K due to the tangential stresses, $\sigma_{\theta\theta}$, is, for $\theta = 90°$;

$$K_M = \left(\frac{2}{\pi a}\right)^{\frac{1}{2}}\sigma_a \int_0^a \frac{[1 + 2A(x/R + 1)^{-2} + 6B(x/R + 1)^{-4}]x^{\frac{1}{2}}}{(a - x)^{\frac{1}{2}}}\,dx \quad (13)$$

where the subscript, M, refers to the mechanical origin of the stress intensity factor. Expanding the reciprocal terms in a series and integrating gives

$$K_M = \sigma_a\left(\frac{\pi a}{2}\right)^{\frac{1}{2}}\left[1 + 2A + 6B - 3(A + 6B)\left(\frac{a}{R}\right)\right] \quad (14)$$

where terms in $(a/R)^2$ etc., have again been neglected. Similarly, for $\theta = 0$,

$$K_M = \sigma_a\left(\frac{\pi a}{2}\right)^{\frac{1}{2}}\left[2A - 6B - 3(A - 6B)\left(\frac{a}{R}\right)\right]. \quad (15)$$

Similar solutions can be obtained for the radial stresses, but since these are small and inhomogeneous complete circumferential cracking is unlikely; hence, they are not considered to play an important role in crack development at inclusions.

4. Crack propagation and arrest

The interface related cracks will start to propagate when K reaches the critical value K_C for either the matrix or the inclusion. This condition can be found by simply substituting the appropriate values for K_C in Equations 8 to 15. Subsequently, however, the crack may arrest if it extends into a *decreasing* stress field. Thus, radial cracks are usually expected to arrest; whereas circumferential cracks may proceed to completion. Consider, as an example, crack propagation through the matrix due to tangential thermal stresses. For $a/R \lesssim 0.2$, Equation 10 can be written in terms of K_C as follows;

$$K = K_C\left(\frac{a}{a_0}\right)^{\frac{1}{2}}\left[\frac{\phi - a/a_0}{\phi - 1}\right] \quad (16)$$

where a_0 is the initial crack length and $\phi = 4R/9a_0$. The K variation represented by this relation is shown in Fig. 4. The important feature to note is that K tends to decrease at large a, resulting in crack arrest (when $K \approx K_C$ [11], at a_a in Fig. 4). The crack extension that occurs prior to arrest, Δa, may be obtained from Equation 16 by solving for a when $K = K_C$. This gives (for $a/R < 0.2$ or $\phi > 2$, the valid regime for this solution);

$$\Delta a = a_0(\phi - 3/4)^{\frac{1}{2}} - \frac{a_0}{2}(3 - 2\phi) \quad (17)$$

Hence, Δa increases as ϕ increases, as indicated in Fig. 4. The size of the crack that forms at the

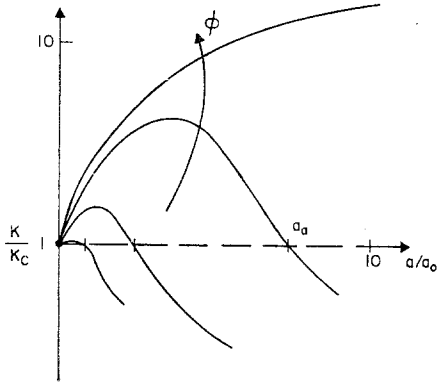

Figure 4 The variation of stress intensity factor, K, with crack length, a, during rapid propagation and arrest, due to propagation in a decreasing stress field.

inclusion due to thermal stresses can thus be found in terms of the initial crack size.

Equivalent solutions for Δa are obtained for the mechanical stresses except that ϕ is given at the critical stress, σ_C, by;

$$\phi = \frac{(1 + 2A + 6B)}{3(A + 6B)} \frac{R}{a_0} \tag{18}$$

for the tangential stress condition with $\theta = 90°$.

5. The incidence of inclusion cracking

Generally it is found that the incidence of cracking at inclusions increases as the inclusion size increases [12], and this feature must be incorporated in the analysis of crack development. The effect of inclusion size on crack formation has previously been explained [12] by noting that the elastic strain energy increases more rapidly with inclusion size than the surface energy needed for complete circumferential cracking; the critical size for cracking is then suggested to occur when these two energies are approximately equal. This approach does not take account, however, of the mechanism for crack development, i.e., that K must exceed K_C at some small flaw in the vicinity of the inclusion matrix interface. An alternative explanation *that relates to the fracture mechanism* is presented in this section.

Some size effect is expected for radial cracking, based simply on the effect of inclusion size on K (Equations 10 and 14). There appears to be an additional size effect, however, because circumferential cracking is also dependent on inclusion size even though K is approximately independent of R (at least when the defects are located at a roughly constant *relative* distance from the interface).

An additional size effect can occur if the interface defects exhibit a statistically related size distribution. Then, the probability, P, that a crack will propagate at a stress, σ, increases as the interface area, A, is increased. If we assume for example that this probability can be fitted to an extreme value distribution of the Weibull type, then;

$$P = 1 - \exp\left[-\left(\frac{\sigma}{\sigma_0}\right)^m \frac{A}{A_0}\right] \tag{19}$$

where σ_0, m and A_0 are system constants. Substituting $A = 4\pi R^2$ and rearranging gives the relative fracture probabilities for two different inclusion sizes, R_1 and R_2, at constant stress;

$$P_2 = 1 - (1 - P_1)^{(R_2/R_1)^2} \tag{20}$$

or, for small P,

$$P_2 = P_1\left(\frac{R_2}{R_1}\right)^2. \tag{21}$$

A substantial effect of inclusion size on the probability of crack development is thus to be anticipated from statistical considerations, e.g., an order of magnitude increase in inclusion size increases the probability by about 10^2.

6. Application to failure prediction

It is common practice with brittle materials to equate the inclusion size ($2R$) to the critical crack size ($2a$), in order to compute the fracture strength (from the stress intensity factor relations). This, it is hoped, will provide at least a conservative estimate of the strength of components containing inclusions. This hypothesis is examined in detail in this section to identify situations where strength overestimates may result.

Generally both the expansion coefficients and the elastic constants will be different for the inclusion and matrix. It is considered for purposes of discussion that the mechanical and thermal stresses superimpose to produce cracking.

When $\alpha_i > \alpha_m$ circumferential cracking is the primary mode of fracture, as mentioned in Section 3.1. Usually the cracks are present in the as-fabricated part due to the thermal stress that develops on cooling from the fabrication temperature; although, occasionally of course, small additional mechanical stresses will trigger the fracture. In principle, circumferential cracks

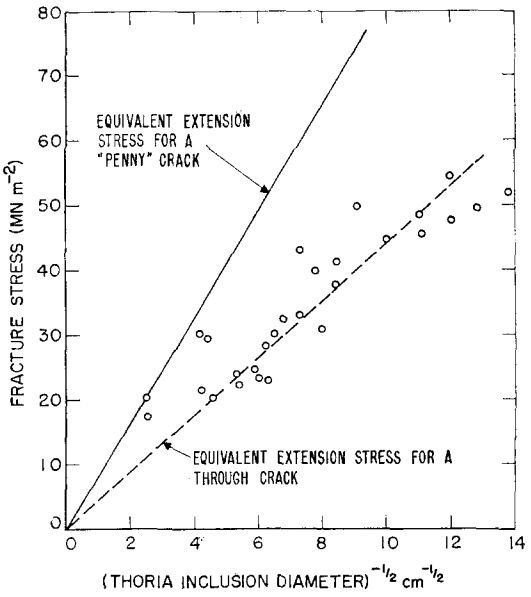

Figure 5 The measured strength of thoria/glass composites [12] compared with the strength calculated by assuming equivalence between the thoria sphere size and "penny crack" size, and sphere size and "through crack" size.

are innocuous, but in practice, the cracks frequently form an incomplete sphere [12]; then it is found that they respond to an applied stress in a manner equivalent to sharp "penny" cracks, approximately equal in size to the inclusion diameter (Fig. 5). The equivalence is not exact, and the departures are more severe for the small inclusions, presumably because the disparity between the crack radius, r, and the inclusion radius, R, increases as R decreases. However, the consequences of equating the inclusion diameter to the crack diameter are not severe, and effective failure prediction can be achieved using, for example, a "correction" factor, $\delta(1 < \delta \lesssim 2)$, to obtain the crack diameter, i.e., $a = \delta R$.

When $\alpha_i \approx \alpha_m$ only the tangential mechanical stresses need be considered. The assumed condition for strength prediction is conservative when $K_M \leqslant K$ (where K is the stress intensity factor for an inclusion sized crack, $K \approx \sigma_a\sqrt{(\pi R)}$) and hence, from Equation 14, when

$$\left(\frac{a}{2}\right)^{\frac{1}{2}}\left[1 + 2A + 6B - 3\left(\frac{a}{R}\right)(A + 6B)\right] \leqslant R^{\frac{1}{2}} \tag{22}$$

or,

$$\left(\frac{a}{R}\right)^{3/2} - \frac{[1 + 2A + 6B]}{3(A + 6B)}\left(\frac{a}{R}\right)^{\frac{1}{2}} + \frac{\sqrt{2}}{3(A + 6B)} \geqslant 0\,. \tag{23}$$

This equation may be solved for a/R (using conventional cubic solutions) to obtain the interface flaw size, a, when $K_M = K$. For flaws larger than this, $K_M > K$ and the strength prediction is no longer conservative. The minimum a which gives $K_M = K$ occurs as $\mu_i \to 0$, and for this condition it is found that $a \approx 0.2\ R$. The interface flaws need to be moderately large, therefore, to cause fracture at a stress below that needed to extend an inclusion sized crack. Normally, flaws of this relative size would be detected during nondestructive inspection (if the inclusion itself is detected). Major problems in failure prediction should not occur, therefore, for this case; although very low modulus inclusions ($\mu_i < 0.1\ \mu_m$) demand careful inspection.

The condition that is liable to present the most difficulty occurs when $\alpha_i < \alpha_m$. Then, tangential stresses develop on cooling from the fabrication temperature. If these stresses lead to the propagation of interface cracks during cooling, these will normally extend a substantial distance from the inclusion before arrest, as discussed in Section 4. These cracks should be detected during nondestructive inspection, e.g. using ultrasonics, and are accountable for failure prediction purposes. However, due to the statistical nature of the interface flaw size and the flaw size dependence of K (Section 5), certain inclusions within the inclusion size range that generally develop cracks will remain uncracked (with the proportion of uncracked inclusions increasing as the inclusion size decreases, Equation 21). The uncracked inclusions can, however, develop cracks during stress application when the mechanical tensile stresses enhance the thermal tensile stresses, i.e., when the modulus of the inclusion is less than the matrix modulus. Superimposing the thermal and mechanical stress (Equations 10 and 14) gives an approximate condition for crack formation due to combined stressing*;

*Note that we have used a cylindrical solution for the mechanical stress and a spherical solution for the thermal stress, so that direct addition of K_M and K_T is not strictly valid; hence, quantitative application of this equation should be avoided.

$$K_S = K_M + K_T \approx \left(\frac{\pi a}{2}\right)^{\frac{1}{2}} \left\{\sigma_a(1 + 2A + 6B) + \frac{\beta}{2} - \left(\frac{a}{R}\right)\left[3\sigma_a(A + 6B) + \frac{9}{8}\beta\right]\right\}. \quad (24)$$

The condition for conservative strength prediction is again found by putting, $K_S < K$, giving

$$\left(\frac{a}{2}\right)^{\frac{1}{2}} \left\{1 + 2A + 6B + \beta/2\sigma_a - (a/R)\,[3A + 18B + 9\beta/8\sigma_a]\right\} < R^{\frac{1}{2}}. \quad (25)$$

This relation shows, for quite modest values of β, that K_M exceeds K at very small a ($\gtrsim 0.01\ R$), especially for low modulus inclusions. Interface flaws in this size range will not be detectable using nondestructive inspection techniques, and gross strength overestimates (assuming inclusion sized cracks) are entirely possible.

It is concluded, therefore, that nondestructive inspection techniques which involve the detection of inclusions (and equate the inclusion size to the crack size) cannot provide effective strength predictions, when the inclusions consist of low modulus and low expansion coefficient material (relative to the matrix). For inclusions of this type, techniques which give a measure of K (or the interface defect size), rather than inclusion size, are the only effective methods for failure prediction, e.g., proof testing [3] and acoustic emission [13]. For high modulus and/or high expansion coefficient inclusions, conservative predictions of failure from inclusions can generally be provided using inclusion size detection techniques, such as ultrasonics and radiography. (Although the possible existence of narrow cracks or incipient cracks, such as improperly bonded zones, may still lead to premature failures.)

7. Examples

Structural applications for brittle materials of substantial current interest are in high temperature gas turbines, high temperature bearings, etc. The two materials which have the most outstanding potential for successful application are silicon nitride and silicon carbide due to their high strength, low expansion coefficient (and hence, good resistance to thermal stress damage) and good strength retention at elevated temperatures. Hence, the effect on strength of the various inclusion types normally detected in these materials, and the potential for failure prediction, are discussed.

Consider first the inclusions in silicon nitride ($\mu = 130$ GN m^{-2}, $\alpha < 4.3 \times 10^{-6}$°C^{-1}). This material can be fabricated to give high strengths using hot pressing procedures [14] (usually with a magnesium oxide additive). The resultant material consists of a fine-grained Si_3N_4 structure with some amorphous phases (due to the reaction of MgO, Si_3N_4 and other impurities), and inclusions introduced during the powder preparation, grinding and hot pressing stages [15]. Since the host material has relatively low values for μ and α, most inclusions will not pose any major problems for conservative failure prediction (presuming, of course, that the inclusions can be identified by nondestructive inspection). The common inclusions in this category are tungsten carbide, boron nitride and silicon carbide [1]. The only potentially problematic inclusions that can currently be identified are those derived from the amorphous phases, Si (Ca, Mg, Al)O_2 [1]. If these phases agglomerate to form inclusions of significant size, then the very low values for α and μ associated with several of the phases could result in extensive crack development and premature failure (unless proof testing and/or acoustic emission can be used for failure prediction, as discussed in Section 6).

Silicon carbide ($\mu = 200$ GN m^{-2}, $\alpha < 5.8 \times 10^{-6}$°C^{-1}) is also prepared in high strength form by hot-pressing, with either aluminium oxide [16] or boron [17] additives. Less is known about the inclusions in these materials, but the larger values of α and μ – compared to silicon nitride – suggest that more problematic inclusion types could be encountered. For example, inclusions of boron carbide, if present, are a potential source of crack development.

8. Conclusions

The stresses that develop around inclusions due to thermal expansion and elastic modulus mismatch are described. The approximate magnitude of the stress intensity factors at interface cracks due to these localized stresses are then evaluated, thereby enabling both the propagation and arrest conditions for these cracks to be estimated. The potential for using nondestructive inspection techniques for failure prediction in components which contain inclusions is then assessed, based on this analysis of the crack propagation condition. It is con-

cluded that inclusion size detection techniques, e.g., ultrasonics, radiography, *may* be adequate for high modulus and/or high expansion coefficient inclusions. For low expansion coefficient and low modulus inclusions, however, these techniques are entirely inadequate and techniques which determine the magnitude of the stress intensity factor, i.e., proof testing and/or acoustic emission, are essential for effective failure prediction.

Acknowledgement

The author wishes to thank the Aeronautics Research Lab for their support of this work, under contract no. F 33615 - 73 - M - 6501.

References

1. Work performed at Westinghouse Laboratories by F. F. LANGE and R. KOSSOWSKY, published in ARPA report, "Brittle Materials Design, High Temperature Gas Turbine," AMMRC CTR73-9 (March 1973).
2. H. R. BAUMGARTNER and D. W. RICHERSON, in "Fracture Mechanics of Ceramics" (Plenum Press, New York, 1974) Vol 1, p, 367.
3. A. G. EVANS and S. M. WIEDERHORN, NBSIR 73-147 (March 1973); *Intl. J. Frac.*, in press.
4. C. F. TIFFANY and J. N. MASTERS, *ASTM STP*, **381** (1964) 249.
5. D. WEYL, *Ber. deut Keram. Ges.* **36** (1959) 319.
6. J. SELSING, *J. Amer. Ceram. Soc.* **44** (1961) 419.
7. M. V. SPEIGHT and R. C. LOBB, *Met. Trans.* **3** (1972) 737.
8. J. N. GOODIER, *J. Appl. Mech.* **1** (1933) 39.
9. P. C. PARIS and G. C. SIH, *ASTM, STP* **381** (1964) 30.
10. S. VAIDYANATHAN and I. FINNIE, *Trans. ASME,* June 1971, p. 242.
11. E. R. FULLER and A. G. EVANS, *Met. Trans.* to be published.
12. R. W. DAVIDGE and T. J. GREEN, *J. Mater. Sci.* **3** (1968) 629.
13. A. S. TETELMAN and A. G. EVANS, in "Fracture Mechanics of Ceramics" (Plenum Press, New York, 1974) Vol. 2, p. 895.
14. R. J. LUMBY and R. F. COE, *Proc. Brit. Ceram. Soc.* **15** (1970) 91.
15. A. G. EVANS and J. V. SHARP, *J. Mater. Sci.* **6** (1971) 1292.
16. Materials produced at Norton Company and Westinghouse, and reported in [1].
17. S. PROCHAZKA and R. J. CHARLES, in "Fracture Mechanics of Ceramics" (Plenum Press, New York, 1974) Vol. 2, p. 579.

Received 31 December 1973 and accepted 7 January 1974.